Microscopic description of the surface dipole plasmon in large Na_N clusters ($950 \lesssim N \lesssim 12\,050$)

Constantine Yannouleas
School of Physics, Georgia Institute of Technology, Atlanta, Georgia 30332-0430
(Received 6 May 1998)

Fully microscopic random phase approximation/local density approximation calculations of the dipole plasmon for very large neutral and charged sodium clusters Na_N^{Z+} in the size range $950 \lesssim N \lesssim 12\,050$ are presented. Sixty different sizes are considered altogether, which allows for an in-depth investigation of the asymptotic behavior of both the width and the position of the plasmon. [S0163-1829(98)06432-7]

The surface dipole plasmon in large metal clusters is currently attracting significant experimental[1–3] and theoretical attention;[4–6] e.g., a time-resolved analysis[1] of second harmonic generation via femtosecond pump-probe studies was recently successful in establishing an upper limit of about 25 nm for the validity of the $1/R$ law[7,8] (where R is the cluster radius) associated with the width of the dipole plasmon in large Na_N clusters. On the theoretical side, this Landau-damping-type width $\Gamma = A\hbar v_F/R$ in large metal clusters has been derived repeatedly with various analytical approaches[7,8] (which necessarily utilize simplified approximations for the dipole matrix elements of the residual Coulomb force), but a microscopic justification of it is still lacking. In general, detailed microscopic studies [the most systematic among them using the matrix–random phase approximation/local density approximation (matrix-RPA/LDA) version[9–12] of the linear response theory] have been restricted to rather small clusters in the size range $8 \lesssim N \lesssim 338$.[10,13]

In the absence of systematic matrix-RPA/LDA calculations above $N = 338$, various other theoretical approaches have been most recently introduced with the expressed purpose of providing a framework for microscopic studies of the dipole plasmon in large metal clusters; they include the in-real-time version of the time-dependent local density approximation,[4,5] the modified-with-separable-residual-forces RPA,[6] and the separation-of-collective-coordinates approach.[5] Due to the computational effort involved, however, these methods were in their turn restricted to a few (about 10) smaller sizes in the range[5] of $8 \lesssim N \lesssim 400$ (or even in the range[6] $8 \lesssim N \lesssim 950$) and as a result they were unable to investigate the asymptotic behavior of the position and the profile of the plasmon. In addition, through an identification of the width with the variance of the RPA response, Kurasawa *et al.*[5] came, via a semianalytical analysis, to the conclusion that the plasmon width should exhibit a $1/\sqrt{R}$ asymptotic dependence, in sharp contrast to the $1/R$ law.

In this paper, with the help of the generation of powerful computers available today, I present systematic matrix-RPA/LDA investigations of the dipole plasma excitation for neutral and charged sodium clusters in the size range $950 \lesssim N \lesssim 12\,050$. In each case 30 different sizes were calculated,[14] which allowed[15] for the determination of the asymptotic size dependence of both the position and the profile of the plasma resonance.

The theoretical aspects of the matrix-RPA/LDA approach have been presented in Ref. 10. Here I only discuss briefly how the matrix-RPA equations [see Eq. 5 of Ref. 10] can be reduced to an equivalent problem with half the dimensions of the original matrix (such a reduction of dimensions is instrumental for the successful implementation of the matrix-RPA/LDA algorithm in the case of the very large metal clusters considered here). For such a reduction, it is sufficient to add and subtract the top and bottom rows of the original matrix equation. One then finds the equivalent equation[16]

$$D(2A^{\lambda} - D)Z^{\nu} = \mathcal{E}_{\nu}^{2} Z^{\nu}, \tag{1}$$

where the matrix A^{λ} is given by Eq. (14) of Ref. 10, λ in general is the multipolarity of the excitation ($\lambda = 1$ for the case of the dipole), $\mathcal{E}_{\nu}$ are the RPA eigenvalues, and D is a diagonal matrix depending exclusively on the unperturbed single particle-hole energies, i.e., $D_{ph,p'h'} = (\epsilon_p - \epsilon_h)\,\delta_{pp'}\delta_{hh'}$. The usual forward- and backward-going RPA amplitudes $W_{+}^{\nu} \equiv X^{\nu}$ and $W_{-}^{\nu} \equiv Y^{\nu}$, which are needed in order to calculate the oscillator strengths f_{ν} (see Sec. II C of Ref. 10), are given through the eigenvectors Z^{ν} as

$$W_{\pm}^{\nu} = \mathcal{C}\left(\frac{\mathcal{E}_{\nu}}{D} \pm 1\right) Z^{\nu}, \tag{2}$$

where the proportionality constant $\mathcal{C}$ is determined via the RPA-eigenvector normalization condition.

For each cluster Na_N^{Z+}, the microscopic RPA calculation yields a discrete set of oscillator strengths f_{ν} (normalized to unity) associated with the RPA eigenvalues $\mathcal{E}_{\nu}$ (see the inset of Fig. 1). By folding the oscillator strengths with Breit-Wigner shapes normalized to unity, one can calculate a smooth photoabsorption cross section σ per valence electron as

$$\sigma(E) = 1.0975(\text{eV Å}^2) \sum_{\nu} f_{\nu} P_{\text{BW}}(E; \mathcal{E}_{\nu}, \gamma_{\nu}), \tag{3}$$

where γ_{ν} denotes the intrinsic widths of the auxiliary Breit-Wigner profiles P_{BW}.

Figure 1 displays the calculated σ's for Na_{952} and $Na_{12\,068}$, namely, for the smallest and the largest size considered in the present paper (intrinsic widths of $\gamma_{\nu} = \gamma = 0.16$ and 0.076 eV were used for Na_{952} and $Na_{12\,068}$, respectively). It is apparent that the full width at half maximum (FWHM) is smaller for $Na_{12\,068}$ ($\sim$ 0.147 eV) compared to the case of Na_{952} ($\sim$ 0.319 eV) and that the maximum of the

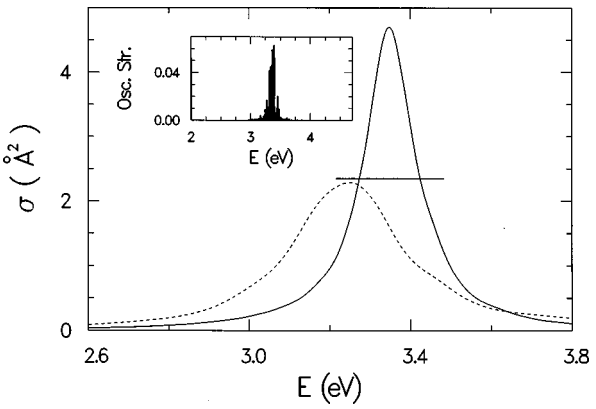

FIG. 1. RPA photoabsortion cross sections for Na_{952} (dashed line) and $Na_{12\,068}$ (solid line). The solid horizontal bar denotes the RPA variance Σ in the case of $Na_{12\,068}$. Inset: the oscillator-strength distribution for $Na_{12\,068}$.

photoabsorption cross section for $N=12\,068$ is blueshifted with respect to the case of $N=952$.

In addition to the photoabsorption profiles, Fig. 1 also displays the variance Σ (horizontal solid bar) associated with the RPA dipole response in the case of $Na_{12\,068}$ [in the RPA the variance is calculated[17] via the relation $\Sigma^2=(m_2/m_0)-(m_1/m_0)^2$, where the moments m_k are given by $m_k=\Sigma_\nu \mathcal{E}_\nu^{k-1} f_\nu$]. Even with the overestimation of the FWHM due to the folding procedure (see below), it is seen that the variance is substantially larger than the corresponding FWHM in the case of $Na_{12\,068}$; thus the variance should not be used as a substitute for the actual width of the dipole plasmon, as was done[18] in Ref. 5. Furthermore, to correct for the overestimation due to the folding, one needs to subtract the intrinsic width γ_ν from the original FWHM (see Fig. 10 of Ref. 10 and accompanying discussion). With this correction, the plasmon widths are $\sim$ 0.16 eV and $\sim$ 0.07 eV for Na_{952} and $Na_{12\,068}$, respectively; these values are even smaller than the uncorrected FWHM's compared to the corresponding variances.

The method of folding described above has been used in most of the earlier publications in order to extract the FWHM of the photoabsorption profiles. This method, however, becomes cumbersome in the present study where the size changes substantially going from the smallest to the largest cluster. Indeed, smaller γ_ν's must be used the larger the cluster size and such a procedure is difficult to be determined uniquely. Instead of the folding method, a more uniform procedure is needed. Using the fact that for large cluster sizes it can be analytically shown[19] that the RPA response itself tends asymptotically to a well concentrated[20] distribution of oscillator strengths f_ν exhibiting a Breit-Wigner profile, i.e.,

$$f_\nu \propto \Gamma/[(\mathcal{E}_\nu-\overline{\mathcal{E}})^2+(\Gamma/2)^2], \tag{4}$$

this paper has opted for a method based directly on the distribution of the f_ν's; namely, the Landau-damping-type width Γ is determined by the minimum interval around the RPA energy centroid $\overline{\mathcal{E}}$, which contains 50% of the total oscillator strength, i.e., Γ is such that $\Sigma_i f_i=0.5$ with $\mathcal{E}_i \in (\overline{\mathcal{E}}-\Gamma/2,\overline{\mathcal{E}}+\Gamma/2)$. The value of 50% used here is precisely

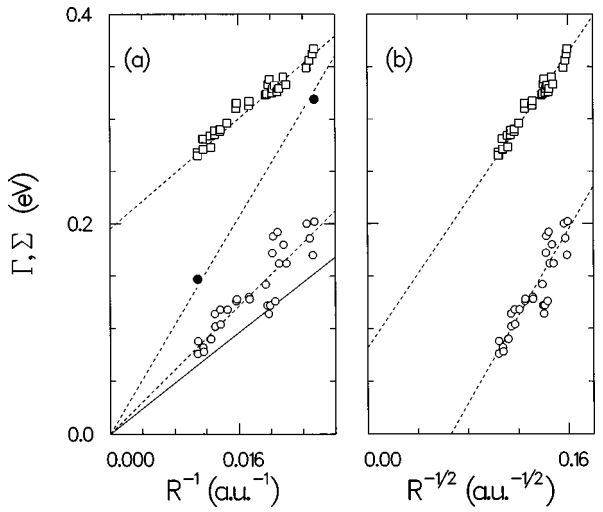

FIG. 2. RPA widths Γ (open circles) and variances Σ (open squares) of the dipole plasmon for neutral Na_N clusters ($952 \leqslant N \leqslant 12\,068$), as a function of (a) the inverse cluster radius $1/R$ and (b) the inverse of the square root of the radius $1/\sqrt{R}$. The solid line in (a) corresponds to the analytical result for Γ according to Ref. 8. The solid dots in (a) denote the *uncorrected* FWHM of the photoabsorption profiles (see Fig. 1) for Na_{952} and $Na_{12\,068}$ generated with the folding method.

the percent of the total oscillator strength contained within the energy interval associated with the FWHM of the single Breit-Wigner profile [see Eq. (4)] and the RPA centroid is given by $\overline{\mathcal{E}}=m_1/m_0$.

Figure 2(a) displays the calculated (according to the latter method) RPA widths (Γ, open circles) and variances (Σ, open squares) for Na_N clusters in the size range $952 \leqslant N \leqslant 12\,068$ as a function of the inverse radius ($1/R$) of the jellium background ($R=r_s N^{1/3}$, and the Wigner-Seitz radius for sodium was taken as $r_s=4$ a.u.). Figure 2(b) displays the same quantities as a function of $1/\sqrt{R}$. Before proceeding further, it needs to be noticed that the corrected FWHM's for Na_{952} and $Na_{12\,068}$ (namely, the values 0.16 and 0.07 eV) according to the folding method are in good agreement with the widths Γ derived from the 50% method.

A first observation is that the variances are systematically larger than the widths (see also Fig. 1). Second, it can be seen that the widths are not proportional to $1/\sqrt{R}$ since the associated straight line does not pass through the origin of the axes [Fig. 2(b)]. On the contrary, in the case of Fig. 2(a), the straight dashed line that passes on the average through the points denoting the widths definitely passes through the origin of axes. This provides an unequivocal proof that $\Gamma \propto 1/R$. Notice that for the smaller sizes the precise values of the widths exhibit noticeable scattering around the average line specified by the $1/R$ law; however, such scattering becomes progressively smaller the larger the cluster sizes. The solid line in Fig. 2(a) denotes the $\Gamma=A\hbar v_F/R$ law according to the analytical result of Ref. 8, namely, when[21] $A=A_{\rm ana}=0.46$. For the numerical RPA calculation, one finds $A_{\rm num}=0.58$, which is close to $A_{\rm ana}$. The difference between the two slopes is due to the infinite-well approximation (and ensuing neglect of electronic spillout), which was invoked during the analytical derivation. To further test the $1/R$ dependence, I have also plotted in Fig. 2(a) the *uncorrected*

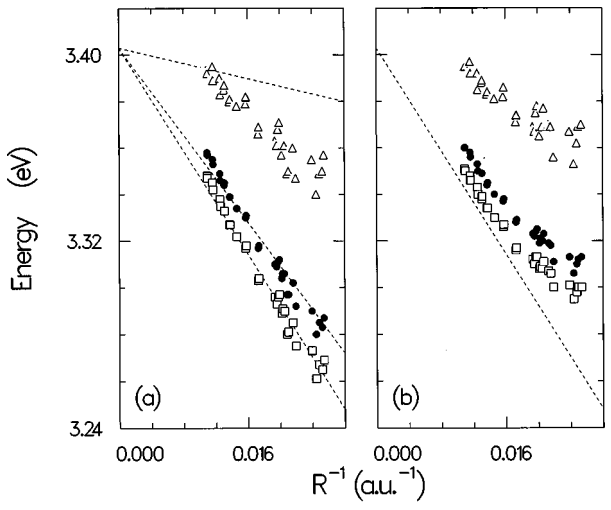

FIG. 3. RPA positional quantities $\mathcal{E}_1$ (open squares), $\overline{\mathcal{E}}$ (centroid, solid circles), and $\mathcal{E}_3$ (open triangles) of the dipole plasmon, as a function of $1/R$ for (a) neutral Na_N and (b) charged Na_N^{10+} clusters. The straight line in (b) is a duplicate of the lowest line in (a) and was drawn as a guide to the eye.

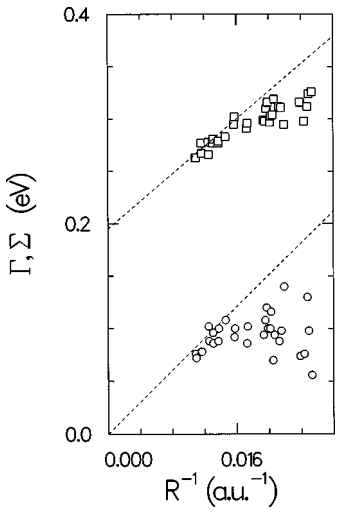

FIG. 4. RPA widths Γ (open circles) and variances Σ (open squares) of the dipole plasmon for charged Na_N^{10+} clusters ($962 \leqslant N \leqslant 12\,078$), as a function of the inverse cluster radius $1/R$. The straight lines are duplicates of dashed lines in Fig. 2(a) and were drawn as guides to the eye.

FWHM's of the photoabsorption profiles for Na_{952} and $Na_{12\,068}$ (solid dots). Again, and in sharp contrast with the variances, even these uncorrected FWHM's follow clearly an $1/R$ dependence.

Finally, it has been derived through semiclassical arguments[5,17] that the size dependence of the variance should be propotional to $1/\sqrt{R}$. Figure 2(b) does not indicate such a relation; much larger sizes are needed before the microscopic results for Σ converge to the expected $1/\sqrt{R}$ relation.

Figure 3 portrays the size evolution of the quantities associated with the position of the RPA surface plasmon, namely, it displays the quantities $\mathcal{E}_1=(m_1/m_{-1})^{1/2}$, $\mathcal{E}_3=(m_3/m_1)^{1/2}$, and the centroid $\overline{\mathcal{E}}$ as a function of the inverse cluster radius. Figure 3(a) corresponds to the case of neutral Na_N clusters, while Fig. 3(b) displays the case of multiply cationic Na_N^{10+} clusters. In all instances, the calculated RPA values honor the theoretically expected[22] inequality $\mathcal{E}_1 \leqslant \overline{\mathcal{E}} \leqslant \mathcal{E}_3$, but the centroid lies much closer to $\mathcal{E}_1$ than to $\mathcal{E}_3$. For the neutral clusters, it is seen that the calculated points for $\mathcal{E}_1$ and $\overline{\mathcal{E}}$ lie closely on two straight lines, which cross the energy axis ($R=\infty$) at about 3.403 eV, in very good agreement with the expected classical Mie limit for sodium clusters, i.e., $\hbar\omega_{\mathrm{Mie}}=\hbar\omega_{\mathrm{bulk}}/\sqrt{3}=3.4$ eV (for $r_s=4$ a.u.). From the relation $\overline{\mathcal{E}}=3.403\ \mathrm{eV}-\overline{\eta}/R$, one can determine $\overline{\eta}=4.68$ (eV a.u.). The calculated points for $\mathcal{E}_3$ do not fall on a straight line crossing the energy axis at about 3.4 eV, although such a behavior has been predicted from semiclassical sum-rule arguments;[17,23] apparently, much larger sizes are needed before the size dependence of $\mathcal{E}_3$ converges to this expected asymptotic behavior.

Comparing the RPA results in Fig. 3(b) with corresponding results in Fig. 3(a), one sees that the position of the dipole plasmon in the case of charged clusters is blueshifted with respect to that of the neutral clusters (all three quantities $\mathcal{E}_1$, $\overline{\mathcal{E}}$, and $\mathcal{E}_3$ exhibit this trend). The extent of this blueshift depends on the ratio Z/N and naturally for the larger charged clusters the calculated positions tend to converge to the corresponding results for the neutral clusters; for $Z=10$, this convergence is definitely recognizable for the largest sizes studied here.

Finally, Fig. 4 displays the size evolution of the RPA widths Γ and variances Σ of the charged Na_N^{10+} clusters as a function of $1/R$. As was the case with the position, the charge state influences the values of Γ and Σ; in particular, a reduction in magnitude of these quantities can be seen compared to the case of neutral clusters. This reduction depends again on the ratio Z/N and it is more pronounced the smaller the cluster size.[24]

In conclusion, fully microscopic RPA/LDA calculations for neutral Na_N and charged Na_N^{10+} ($950 \lesssim N \lesssim 12\,050$) clusters were presented. In each case, some 30 different sizes were considered, which allowed for an in-depth investigation of the asymptotic behavior of both the position and the width of the dipole plasmon. In particular, it was found that asymptotically the RPA width becomes proportional to the inverse cluster radius and that for neutral clusters this trend is already well developed within the size range considered here.

Computations were performed at the GIT Center for Computational Materials Science.

[1] J.-H. Klein-Wiele, P. Simon, and H.-G. Rubalin, Phys. Rev. Lett. **80**, 45 (1998).
[2] D. Steinmüller-Nethl *et al.*, Phys. Rev. Lett. **68**, 389 (1992).
[3] P. Markowicz, K. Kolwas, and M. Kolwas, Phys. Lett. A **236**, 543 (1997).
[4] K. Yabana and G. F. Bertsch, Phys. Rev. B **54**, 4484 (1996).
[5] H. Kurasawa, K. Yabana, and T. Suzuki, Phys. Rev. B **56**, 10 063 (1997).
[6] V. O. Nesterenko *et al.*, Phys. Rev. A **56**, 607 (1997).
[7] U. Kreibig and M. Vollmer, *Optical Properties of Metal Clusters* (Springer-Verlag, Berlin, 1995); A. Kawabata and R. Kubo, J. Phys. Soc. Jpn. **21**, 1765 (1966).
[8] (a) C. Yannouleas and R. A. Broglia, Ann. Phys. (N.Y.) **217**, 105 (1992); (b) C. Yannouleas, Nucl. Phys. A **439**, 336 (1985).
[9] C. Yannouleas *et al.*, Phys. Rev. Lett. **63**, 255 (1989); Phys. Rev. A **44**, 5793 (1991).
[10] C. Yannouleas, E. Vigezzi, and R. A. Broglia, Phys. Rev. B **47**, 9849 (1993).
[11] C. Yannouleas, Chem. Phys. Lett. **193**, 587 (1992).
[12] C. Yannouleas, F. Catara, and N. Van Giai, Phys. Rev. B **51**, 4569 (1995).
[13] Some matrix-RPA/LDA calculations for cluster sizes with $N>338$ have also been reported, e.g., for the case (Ref. 12) of Na_{952} and the case (Ref. 8) of Na_{1982}. F. Catara *et al.* [Z. Phys. D **33**, 219 (1995)] have also reported matrix-RPA/LDA calculations for five Na_N clusters in the size range $1300 \lesssim N \lesssim 5500$.
[14] In the case of neutral (charged) clusters, Na_{952} (Na_{962}^{10+}) was the smallest and $Na_{12\,068}$ ($Na_{12\,078}^{10+}$) the largest cluster studied. In all instances, a spherical jellium background was assumed for simplicity. The energy-weighted sum rule was fulfilled with a better than 0.1% accuracy.
[15] Due to the small number of points and the low size range, as well as to numerical inaccuracies, Catara *et al.* (see Ref. 13) were unable to study *microscopically* the asymptotic behavior of the plasmon width and position. In particular, the subject of the plasmon width was omitted altogether, while the study of the asymptotic position was based (see their Eq. 14) on a sum-rule determination of the upper bound $\mathcal{E}_3$ (see below) in conjunction with a Woods-Saxon–type estimate of the electronic spillout. Their numerical inaccuracies have been reflected in the fact that the plasmon peak positions become larger than the theoretical upper bounds $\mathcal{E}_3$ ($\overline{E}_1^{\mathrm{JM}}$ in their notation) above $N \sim 2654$ (see their Table 3).
[16] In the derivation of Eq. (1), the relation $A^\lambda - D = (-1)^\lambda B^\lambda$ (valid in the case of the Coulomb residual force) was used to eliminate the RPA submatrix B^λ.
[17] M. Brack, Phys. Rev. B **39**, 3533 (1989).
[18] Under the appearance of the Tomonaga theory, it seems that Ref. 5 has rediscovered the celebrated *generalized Kohn theorem* [L. Brey *et al.*, Phys. Rev. B **40**, 10 647 (1989)], which states that, in the case of a perfect parabolic confinement, the center-of-mass motion of the electron gas separates completelety from the intrinsic motions. Reference 5 overlooked the fact that, although the absence of electronic spillout is a *necessary* condition whenever this theorem applies, it is by no means a *sufficient* one. For example, J. Dempsey *et al.* [*ibid.* **47**, 4662 (1993)] have shown that, in the case of an overfilled quantum well, Landau damping is present even though the electronic spillout is negligible due to the hard-wall potential utilized (see their Sec. III B 1). Rather than the electronic spillout, the crucial factor for the appearance of Landau fragmentation is whether the electronic density ''feels'' the nonparabolic part of the confining potential. For the relevance of the generalized Kohn theorem to the case of highly cationic metal clusters, see Sec. II B of Ref. 12.
[19] See C. Yannouleas, M. Dworzecka, and J. J. Griffin, Nucl. Phys. A **379**, 256 (1982), in particular Secs. 3.2, 3.3, and 3.4; see also Sec. 5 of Ref. 8(a).
[20] For small clusters, e.g., Na_8, Na_{20}, and Na_{40}, the fragmentation of the oscillator strength can be irregular and can lead to the appearance of multipeak photoabsorption profiles (see Refs. 9 and 10).
[21] A_{ana} depends on the ratio of the surface-plasmon energy over the Fermi energy [see Eq. 66 of Ref. 8(a)].
[22] Derived from general sum-rule arguments, see, e.g., O. Bohigas, A. M. Lane, and J. Martorell, Phys. Rep. **51**, 267 (1979).
[23] No such closed semiclassical asymptotic behavior has been derived for $\mathcal{E}_1$ and $\overline{\mathcal{E}}$.
[24] A similar dependence of the plasmon width (and of the position as discussed earlier) on the charge state was also found in the case of small clusters with $N - Z \leqslant 40$ (see Refs. 9, 11, and 12).